ELSEVIER

Coastal Engineering 28 (1996) 93–120

COASTAL ENGINEERING

A new non-dimensional number for the analysis of wave reflection from rubble mound breakwaters

M.A. Davidson [a,*], P.A.D. Bird [a], G.N. Bullock [a], D.A. Huntley [b]

[a] School of Civil and Structural Engineering, University of Plymouth, Palace St., Plymouth, Devon, UK
[b] Institute of Marine Studies, University of Plymouth, Drake Circus, Plymouth, Devon, UK

Received 2 May 1995; accepted 9 February 1996

Abstract

Full scale measurements of the reflection performance of a rock island breakwater were obtained using an array of 6 pressure transducers, both before and after a reduction of the seawards slope of the structure. This slope reduction (1 : 0.82 to 1 : 1.55) effectively reduced maximum reflection coefficients by 15%. Comparisons of reflection coefficients with various surf-similarity parameters including the Iribarren and Miche numbers failed to provide an accurate parameterization of wave reflection for both data sets. Multiple regression analysis indicated that the shortcomings of the available surf-similarity parameters can be attributed to an overemphasis of the effects of the incident wave height (H_i) and the structure slope ($\tan\beta$) relative to the wavelength (L). On the basis of the regression analysis a new non-dimensional reflection number $R = d_t L_0^2 \tan\beta / H_i D^2$ is postulated here, which revises the relative weightings of these parameters, and introduces other physically significant parameters, including the local water depth at the toe (d_t), and the characteristic armour diameter (D). This reflection number more effectively parameterizes wave reflection for these data, and for the first time provides the basis for a new scheme for the prediction of reflection coefficients (K_r) based entirely on the analysis of full scale data, where; $K_r = 0.151 R^{0.11}$ or $K_r = 0.635\sqrt{R}/(41.2 + \sqrt{R})$.

1. Symbols

a	empirical coefficient
b	empirical coefficient
c	constant of proportionality (multiple regression analysis)
d	local mean water depth measured vertically upwards from the sea bed

* Corresponding author.

PII S0378-3839(96)00012-9

d_t	mean water depth measured at the toe of the structure
D	characteristic diameter of rock armour $(W_{50}/\rho)^{1/3}$
$E_i(f)$	incident wave energy spectral estimate
$E_r(f)$	reflected wave energy spectral estimate
f	frequency
f_p	spectral peak frequency
g	acceleration due to gravity
H_b	wave breaker height $(=0.17L_0\{1-\exp[-4.712(d_t/L_0)(1+15m^{1.33})]\})$ (Goda, 1975)
H_i	Incident wave height
k	wave number $(=2\pi/L_p)$
$K_r(f)$	frequency dependent reflection coefficient
K_r	frequency averaged reflection coefficient, $K_r = \sqrt{\int_{f=0.05\,\mathrm{Hz}}^{f=0.4\,\mathrm{Hz}} E_r(f)\mathrm{d}f \Big/ \int_{f=0.05\,\mathrm{Hz}}^{f=0.4\,\mathrm{Hz}} E_i(f)\mathrm{d}f}$
L_p	wavelength corresponding to f_p given by linear wave theory
L_0	deep water wavelength $(g/2\pi f_p^2)$
m	offshore gradient seawards of the structure
M	Miche number
p	power law dependence (multiple regression analysis)
P	notional permeability (Van der Meer, 1988)
R	reflection number $(=d_t L_0^2 \tan\beta/H_i D^2)$
r	correlation coefficient (multiple regression analysis)
T_p	peak wave period $(=1/f_p)$
U_r	Ursell number
v_t	shallow water wave velocity at the toe $=\sqrt{gd_t}$
$\bar{v}$	average shallow water wave velocity over the breakwater slope $=\frac{2}{3}\sqrt{gd_t}$
W_{50}	median mass of rock armour
X	primary or secondary variable (multiple regression analysis)
z	depth measured vertically upwards from the still water level
α	angle of wave approach measured relative to a line normal to the shoreline
$\tan\beta$	structure gradient
$\gamma(f)$	coherence spectrum
ξ	Iribarren number computed using deep water wavelength $(=\tan\beta/(H_i/L_0)^{0.5})$
ξ_p	Iribarren number computed using L_p, $(=\tan\beta/(H_p/L_0)^{0.5}$
ρ	rock armour density
σ	standard error in multiple regression analysis

2. Introduction

The problems associated with the reflection of incoming waves from coastal structures and natural coasts are well recognised. The detrimental effects of wave reflection include; intensified sediment scour, which can lead to a dramatic loss in beach material and the destablization of structures, and dangerous sea states near the entrances to harbours.

Due to the adverse effects of wave reflection the coastal engineer requires design criteria which enable cost effective structures to be built with acceptable reflection performances. This fact has prompted numerous theoretical and model scale studies of wave reflection which have yielded a variety of predictive schemes. However, to date there have been relatively few full-scale measurements of wave reflection. It remained to be seen therefore whether design criteria based on theoretical studies and model scale tests were valid at full scale.

This paper details a comprehensive assessment of the reflection performance of a full-scale rock island breakwater. Measurements were obtained under a broad range of incident wave conditions, both before and after a modification to the seawards slope of the structure. These data provide a unique opportunity to examine existing wave reflection models for permeable slopes at full scale, assess the sensitivity of the reflection performance of the breakwater to structure slope and to develop an improved predictive scheme for wave reflection from rock island breakwaters.

Firstly, a brief review is given of the equations currently available to the coastal engineer for the prediction of wave reflection. This is followed by a description of the field site, instrumentation and a summary of the wave climate during the experiment. Specific details are given of the analysis procedure, definition of parameters used in this paper and sources of potential errors. Analysis of field data is used to develop an improved parameterization of wave reflection and a predictive scheme based entirely on full scale measurements.

3. Predictive schemes for wave reflection

3.1. Wave reflection from smooth-impermeable slopes

Miche (1951) empirically determined that the reflection coefficient for monochromatic waves which are steep enough to break on a plane beach of gradient $\tan\beta$ will be proportional to the ratio of the critical wave steepness to the incident wave steepness. According to this hypothesis the reflection coefficient (K_r) will be proportional to a Miche number (M) of the form:

$$K_r \propto M = \frac{4g}{(2\pi)^{5/2}} \frac{\tan^{5/2}\beta}{(H_i f^2)} \quad \text{and} \quad K_r = 1 \;\text{ for }\; M \geq 1 \tag{1}$$

Ursell et al. (1960) and Seelig and Ahrens (1981) presented model scale tests that indicated that Miche's equation significantly overestimated the reflection of both regular and irregular waves from smooth slopes.

Battjes (1974, 1975) redefined Miche's hypothesis in terms of a surf-similarity parameter known as the Iribarren number ($\xi = \tan\beta/(H_i/L_0)^{0.5}$), yielding the following expression for the reflection coefficient:

$$K_r = 0.1\xi^2 \tag{2}$$

Laboratory tests with random waves (Ahrens, 1980) indicated that Battjes' equation provided more accurate estimates of K_r than Miche's equation (Eq. 1) when waves were steep enough to break on the slope but still overestimated K_r for $\xi > 3$. Seelig and Ahrens (1981) found improved estimates of K_r over a wider range obtained from the equation

$$K_r = \frac{a_1 \xi^2}{b_1 + \xi^2} \tag{3}$$

where a_1 and b_1 are empirical coefficients with values of 1.0 and 6.2 respectively for smooth slopes. Equations 1, 2 and 3 indicate that the principle factors affecting wave reflection from smooth slopes include wave frequency (linked to wavelength via the dispersion equation), wave height and structure slope.

3.2. Wave reflection from rough-permeable slopes

Wave reflection from permeable structures is also a function of porosity which augments transmission, and surface roughness which increases dissipation. Seelig and Ahrens (1981) presented a comprehensive review of the available laboratory data for smooth slopes (Ahrens, 1980; Ursell et al., 1960), rough-impermeable slopes (Ahrens and Seelig, 1980; Madsen and White, 1976; Moraes, 1970; Seelig and Ahrens, 1981), rough-permeable slopes (DeBok and Sollitt, 1978; Gunbak, 1979; Seelig, 1980; Hydraulics Research Station, 1970) and laboratory beaches (Chesnutt, 1978). Based on the available data for rough-permeable slopes Seelig and Ahrens (1981) found that Equation 3 with a_1 and b_1 set equal to 0.6 and 6.6 respectively, provided a conservative estimate for wave reflection for which 95% of the available laboratory data fell below. These data also indicated that the reflection coefficient reduction factor a_1 which defines the upper saturation value of K_r is a function of wave breaking at the toe or seawards of the structure, surface roughness and the number of armour layers.

Thus, in addition to the parameters L (or f), H, and $\tan\beta$ which control wave reflection from smooth slopes, Seelig and Ahrens postulated that wave reflection from porous structures is also a function of the depth at the toe (d_t), the slope of the seabed offshore of the structure (affecting wave breaking offshore), the characteristic diameters of the armour (D, affecting surface roughness) and the number of layers of armour. Recommendations based on Seelig and Ahrens results are included in the US Army Shore Protection Manual (1984).

Allsop (1990) conducted random wave laboratory tests on breakwaters with one and two layers of rock armour and found a good agreement with Eq. 3 with best fit values of $a_1 = 0.64$, $b_1 = 7.22$ (one armour layer) and $a_1 = 0.64$, $b_1 = 8.85$ (two armour layers).

Giménez-Curto (1979) suggested an alternative exponential model for wave reflection also based on the Iribarren number:

$$K_r = a_2[1 - \exp(b_2 \xi_{\mathrm{r.m.s.}})] \tag{4}$$

Here the r.m.s. incident wave height must be used to compute ξ for random waves (Losada, pers. commun.). Best-fit analysis with the laboratory data of Sollitt and Cross

(1972) for a rubble mound structure give values for the empirical coefficients a_2 and b_2 of 0.503 and -0.125 respectively (Losada and Giménez-Curto, 1981).

Numata (1976) reported the results of laboratory tests on a vertical, permeable, non-overtopped breakwater comprised of artificial concrete blocks. Numata suggested another empirical equation for wave reflection based on the ratio of breakwater width to armour diameter:

$$K_r = a_3\left(\frac{\text{Breakwater Width}}{\text{Armour Diameter}}\right)^{b_3} \tag{5}$$

Again a_3 and b_3 are empirical coefficients which are a function of the relative depth at the toe (d_t/L_0). Numata's equation suggests a direct relationship between reflection coefficient and breakwater width which determines the transmission of wave energy through the structure. The effect of increasing armour diameter is two fold. Firstly, the roughness of the structure is increased promoting dissipation due to friction and turbulence, and secondly, the void area (αD^2) between the blocks is increased, thus, enhancing transmission.

Postma (1989) conducted 300 random-wave flume tests on rock slopes, independently examining the effects of f, H, $\tan\beta$, d_t, notional permeability P (see Van der Meer, 1988 for a definition of P), gradation and spectral shape on K_r. This analysis revealed a strong dependence of K_r on f, $\tan\beta$, and permeability, a weaker dependency on H, and negligible correlations with spectral form and depth at the toe. Postma analysed his data together with that of Allsop and Channell (1988) to give an empirical equation similar in form to Battjes' equation where:

$$K_r = 0.125\xi^{0.73} \tag{6}$$

Van der Meer (1992) comments that the Iribarren number does not accurately describe the combined effect of slope and wave steepness and that an improved fit to Postma's data can be achieved using multiple regression analysis and separating these parameters. This analysis results in an empirical equation of the form:

$$K_r = 0.071 P^{-0.082} \tan^{0.62}\beta\left(\frac{H_i}{L_0}\right)^{-0.46} \tag{7}$$

This brief review highlights parameters which influence wave reflection and the wide range of empirical predictive equations available to the coastal engineer, all of which are based on laboratory tests. At present none of these equations have been adequately tested at full scale. However, some large scale laboratory tests have been conducted. Oumeraci and Partensky (1990) and Muttray et al. (1992) conducted large scale tests using tetrapods and accropods respectively. Both workers found a reasonable agreement between reflection measurements and Eq. 3. It is interesting to note however, that Oumeraci and Partensky's large scale tests on tetrapods give empirical coefficients which indicate significantly larger (25%) maximum levels of reflection ($a_1 = 0.6$) than Allsop's and Hettiarachchi's (1988) small scale tetrapod tests ($a_1 = 0.48$) over a similar range of Iribarren numbers. Conversely, large scale model tests by Sollitt and DeBok (1976), Shimada et al. (1986) and Postma (1989) indicate that reflection coefficients are likely to vary by less than 10% between model and full scale. The precise effects of scale still require further investigation.

4. Site description and measurement programme

Sea surface elevation measurements were obtained in a reflective wave field seawards of a low crested rubble-mound breakwater of reef type at Elmer, West Sussex, UK (Fig. 1, Fig. 2a and b). A full description of the site and details of construction may be found in Holland and Coughlan (1994) and Bird et al. (1995).

The original structure, constructed in 1991/92 consisted of 4–8 tonne carboniferous limestone blocks with a design gradient of 1 : 1. The stability of this provisional structure was improved in 1993 by the addition of 6–10 tonne syonite blocks to its seaward face. This reduced the design gradient of the seawards slope to 1 : 2. Although the overall design conditions were satisfied, detailed surveys of the rubble mound over a 10m length of the structure immediately shorewards of where the measurements were taken indicated local (effective) reflection surfaces with average slopes of 1 : 0.82 and 1 : 1.55 for the preliminary and modified structure respectively. Wave measurements were obtained from the same location both before and after the breakwater modifications. Hereafter the pre- and post- modification data-collection exercises will be referred to as deployment 1 (or dep. 1) and deployment 2 (or dep. 2) respectively.

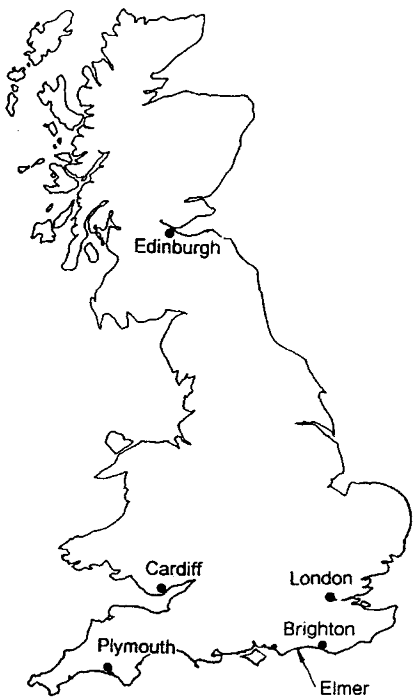

Fig. 1. Location map.

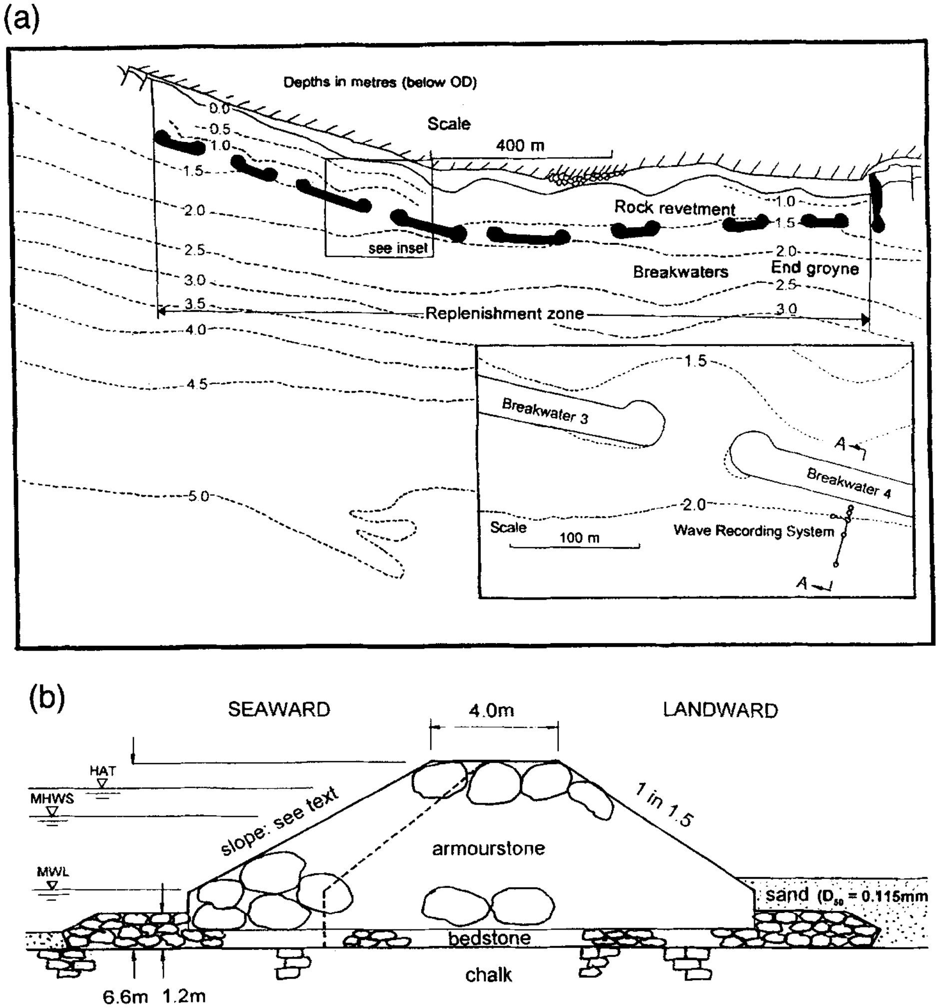

Fig. 2. (a) Plan of the breakwater scheme, showing the layout of instrumentation. (b): Section A–A through the breakwater at the recording site.

Transmission of wave energy through over-topping is limited to periods of high tide which occur simultaneously with extreme storm conditions (such conditions did not arise during the measurement period).

Wave measurements were obtained using a purpose built wave recorder system consisting of a series of 6 pressure transducers connected to a central signal conditioning and data storage unit via armoured cables. The transducer array consisted of 5 pressure transducers spaced along a line 45 m long running directly offshore at right angles to the breakwater (sensors spacing = 3 m, 6 m, 12 m and 24 m), and a sixth transducer offset 12 m in the longshore direction from the main cross-shore transect (Fig. 2a). The first transducer was positioned a distance of approximately 5 m from the toe of the structure.

Table 1
Summary of conditions during field data collection (a full definition of parameter definitions is given in Section 5)

Parameter	Dep. 1	Dep. 2
d_t (m)	0.99–4.62	1.15–4.56
H_i (m)	0.06–1.64	0.15–1.47
Peak period T_p (s)	3–19	4–15
ξ	6.4–70.7	4.4–23.1
Ursell No. U_r	< 1	< 1
$\tan\beta$	1.23	0.64
D (m)	1.38	1.44
d_t / gT_p^2	0.0005–0.5053	0.0029–0.8886
D / d_t	0.229–1.398	0.316–1.258
D / L_0	0.016–0.145	0.015–0.079
H_i / H_b	0.028–0.436	0.067–0.479

Data from all 6 transducers were logged simultaneously at 2 Hz, and records were taken every 3.1 hours. A more detailed discussion of the wave recorder system is given in Bird and Bullock (1991) and Bird et al. (1994).

586 records were collected during the first deployment prior to the breakwater modification (June to August 1992), and 364 records were obtained after the slope reduction (February to April, 1994). A summary of the range in wave conditions sampled during these field deployments and details of the structure are given in Table 1. A number of dimensionless variables have been included in Table 1 for ease of comparison of this study with other field and laboratory tests.

5. Selected procedure for data analysis

An important aspect of this research is the development of an improved predictive scheme for wave reflection from rock island breakwaters. It is necessary therefore to define with some clarity how each of the parameters used here are calculated. This section gives a detailed outline of the analysis procedure and a discussion of the potential sources of error in the measurement of wave reflection.

Seabed pressure time-series collected from the 6 spatially separated pressure transducers (Fig. 2a) consisting of 6×1352 data points were de-meaned, de-trended, and divided into 2 overlapping segments 1024 data points in length. A Hanning window was applied to each of the data segments which were subsequently Fourier transformed and used to form a cross-spectral density matrix. Data were smoothed by ensemble averaging the transformed data segments and further frequency averaging 5 data points. The resulting bandwidth of the frequency bins was 0.0098 Hz.

The pressure spectra were then converted to estimates of surface elevation through the application of a frequency domain weighting function given by linear wave theory. The resulting cross-spectral density matrix (between different sensors) was then used to decompose the measured wave field into incident and reflected wave spectra using an algorithm detailed by Gaillard et al. (1980). This 2-dimensional, linear analysis technique is based on a method first derived by Kajima (1969) which operates on a pair of spatially separated sensors. However, Kajima's original algorithm is subject to singularities when the sensor spacing is equal to an integer number of half wavelengths. The method of Gaillard et al. (1980) is designed to operate on 3 unequally spaced sensors and introduces a mathematical weighting function which eliminates the singularities in Kajima's original solution. It was found that the most stable estimates of the frequency dependent reflection function ($K_r(f) = \sqrt{E_r(f)/E_i(f)}$) were obtained using the sensor triplet with minimum spatial separations in order to maximise the coherency of the signal between sensor pairs.

5.1. Definition of reflection parameters

The frequency averaged reflection coefficient was computed by summing the decomposed incident and reflected wave spectra over the limits of the gravity band (taken to be 0.05 Hz to 0.4 Hz, so that wave periods between 20 s and 2.5 s were embraced):

$$K_r = \sqrt{\frac{\int_{f=0.05\,\mathrm{Hz}}^{f=0.4\,\mathrm{Hz}} E_r(f)\,\mathrm{d}f}{\int_{f=0.05\,\mathrm{Hz}}^{f=0.4\,\mathrm{Hz}} E_i(f)\,\mathrm{d}f}} \tag{8}$$

For these data measured infragravity energy (< 0.05 Hz) was low and in all cases subordinate to incident band oscillations. Spectral energy levels in the seabed pressure above 0.4 Hz were also negligible.

The process of wave reflection is often measured relative to the Iribarren number, $\xi = \tan\beta/\sqrt{(H_i/L_0)}$. Here, L_0 is the deep water wavelength ($= g/2\pi f_p^2$) defined for the spectral peak period (f_p), and H_i is the incident wave height calculated from the decomposed incident wave spectrum as follows:

$$H_i = 4\sqrt{\int_{f=0.05\,\mathrm{Hz}}^{f=0.4\,\mathrm{Hz}} E_i(f)\,\mathrm{d}f} \tag{9}$$

The value of H_i was found to be insensitive to offshore location due to the shallow sloping sea bed (gradient < 0.02) on which the pressure sensors were located (wave shoaling offshore of the breakwater is negligible). This quantity is therefore equivalent to the incident wave height evaluated at the toe of the structure, outside the breaker zone, since the depth change between the sensors and the breakwater is minimal (< 0.1 m) and in all records analysed here wave breaking occurred on the structure.

A second non-dimensional parameter which gives a quantitative measure of the linearity of the waves is the Ursell Number (Guza and Thornton, 1980):

$$U_r = \frac{H_i}{2d_t(kd_t)^2} \tag{10}$$

Again this quantity is evaluated at the toe of the breakwater (depth at the toe $= d_t$) with

$k = 2\pi/L_p$. Inspection of incident wave spectra revealed the presence of well defined harmonics of the primary spectral peak for all records for which $U_r > 1$. Therefore, all data exhibiting strong non-linearities (i.e. $U_r > 1$) were not included in the analysis described here in order to preserve accuracy in the linear analysis technique.

Encouragingly, tests carried out on field data indicated that estimates of the significant incident wave height and reflection coefficient derived from any of the 10 possible sensor triplets in the cross-shore array (of 5 sensors) were very consistent. Typical standard deviations in K_r estimates for different sensor triplets were < 0.01 during long crested wave conditions. Incident wave height estimates showed similarly small deviations ($< 1\%$) for different sensor triplets confirming that wave shoaling over the length of the array was minimal.

Larger variations in K_r (> 0.05) estimates from different sensor triplets were observed during irregular, short wind wave conditions, due to low coherency of the measured signals from sensors with higher spatial separations. Careful design of the wave recorder system (Bird and Bullock, 1991) ensured very low levels of instrument noise (dominated by quantisation noise due to the resolution which was set at 100 Pa). However, low coherency ($\gamma(f)$) between sensor pairs may still occur as a result of the following:

1. The dominance of highly irregular wave motions ("surface chop") forced by strong local winds. Perturbations such as these are seldom coherent from one sensor to the next.
2. The presence of strong nodal regions due to phase-locking of incident and reflected waves.
3. Very low signal energy (e.g. at $f > 0.4$ Hz).

Intensive numerical tests were employed in order to establish data rejection criterion for incoherent data, and to establish the potential errors resulting from oblique wave incidence. These tests indicated that for the given array geometry and average water depth the error in K_r due to the combined effect of low coherence ($0.8 < 1.0$) and oblique wave approach ($0° < \alpha < 25°$) were $< \pm 0.09$ for $0.4 < K_r < 1.0$.

These numerical tests combined with visual inspection of time series and spectral data lead to the following data quality/acceptance criteria:

- Ensure some significant wave activity: $H_i > 0.05$ m.
- Ensure the sensors do not dry out at any time during the data run: $d > (z + d) + H_i$.
- Eliminate strongly non-linear data: $U_r < 1$.
- Minimise errors in K_r estimates due to low signal coherence: $\gamma(f) \geq 0.8$ between all 3 sensor pairs in the analysis triplet (eliminates data points not the whole data file).
- Bimodal or multi-peaked incident wave spectra were eliminated. Examples of bimodal spectra include those with both significant swell and local wind generated sea components. Computation of parameters such as the Iribarren number require the offshore wavelength corresponding to the spectral peak frequency which is highly ambiguous with these irregular, multipeaked spectra. Identification of these data was most effectively achieved via visual inspection.

All data were entered into a data base, which conveniently allowed data to be isolated in accordance with specific criteria. Those data which failed any of the above quality control tests were identified with a numeric flag which indicated that the data should be neglected from further analysis and which of the above 5 criteria above had not been satisfied.

6. Results

6.1. Structure slope

One of the primary concerns of this paper is the sensitivity of wave reflection to variations in structure slope. However, the assessment of an appropriate value for the structure slope of an irregular rubble mound structures is not trivial. An estimate of structure slope may vary greatly depending on which profile line is selected for analysis. In order to evaluate an appropriate value for the "effective" structure slope an extensive electronic distance meter (EDM) survey of the structure was undertaken. This consisted of several profiles of the breakwater taken over a frontage that extended 5 m either side (alongshore) of the wave recorder array location. Linear regression analysis of these data was used to evaluate the average gradient for the seawards face of the structure corresponding to the area opposite the wave recorder array, (see Table 1 for slope values). Results of the EDM survey for deployment 2 are given by the open squares in Fig. 3. There is some scatter in the data which is of the order of the representative diameter of the mound material (1.44 m).

A further independent survey of the same breakwater area carried out in accordance with CIRIA/CUR (1991) guidelines using a staff fitted with a hemispheric foot agreed closely to the EDM survey to within 2°. The excellent agreement between these 2 profiling techniques indicates that the breakwater gradient estimates are both accurate and reproducible.

Also shown in Fig. 3 (by the crosses) are the locations of breakwater reflections which were "remotely sensed" by the wave recorder array. The reflection point location was calculated here using a method first outlined by Gaillard et al. (1980) which enables the computation of a complex frequency domain transfer function relating incident and reflected wave spectra. The magnitude of this transfer function is equivalent to the frequency dependent reflection coefficient and the phase corresponds to the phase angle between the incident and reflected waves at an arbitrary reference location (e.g. one of the transducers). Combining the phase angle between the incident and reflected waves $\phi(f)$ with the known wavelength $L(f)$ (given by the linear dispersion equation) allows the reflection point distance (rpd) of the waves to be evaluated relative to the arbitrary reference location, where rpd $= L(f)\phi(f)/4\pi$. This simple calculation assumes; normal wave incidence, a flat sea bed, and a vertical reflector. However, if the structure and/or the sea bed are sloping the apparent reflection point distance appears to be shorewards of the reflecting surface of the structure as a consequence of wave shoaling and a correction must be applied. In this example (Fig. 3) a correction (Δx) to the reflection point distance for wave shoaling over the structure has been derived using shallow water linear wave theory and added to the rpd estimate. Δx is directly related to the water depth and inversely related to the structure gradient, where $\Delta x = d_t(\bar{v} - v_t)/(\bar{v}\tan\beta)$. Here v_t is the phase velocity at the breakwater toe $= \sqrt{gd_t}$ and $\bar{v}$ is the average velocity

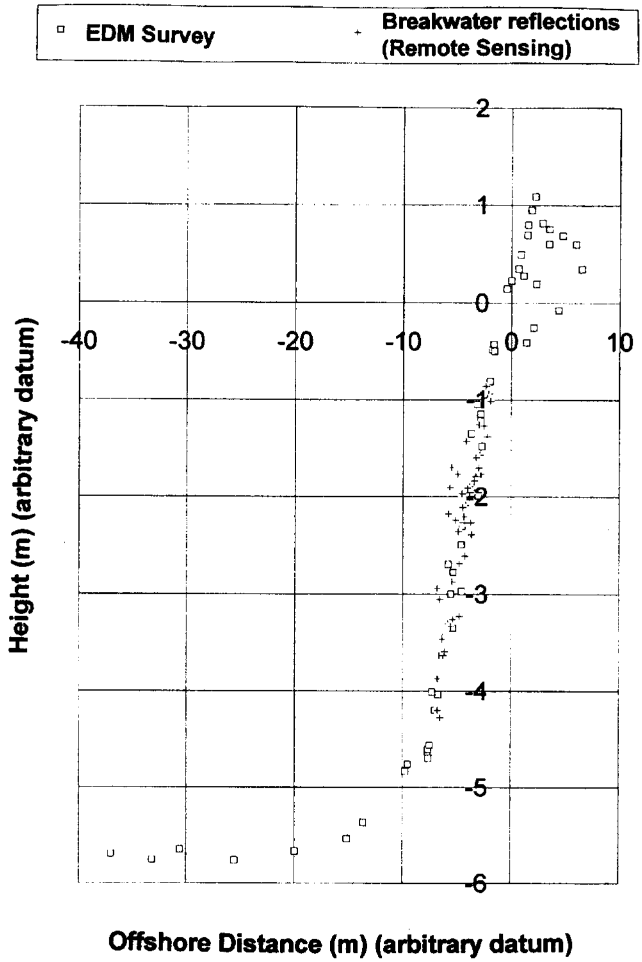

Fig. 3. Electronic distance meter survey showing a cross-section of the seawards face of the breakwater and part of the beach. Also shown are the breakwater reflections, remotely sensed by the pressure transducer array.

over the sloping breakwater $= \frac{2}{3}\sqrt{gd_t}$. Estimates of the reflection point distance were obtained for each frequency bin in the energetic region of the spectrum and an average value obtained. Ambiguities in the rpd estimates equal to an integer number of half wavelengths may occur if the array is located a distance of $> L(f)/2$ away from the reflection point. These errors a easily noticeable and can be simply corrected.

Inspection of Fig. 3 shows a good agreement between the EDM survey data and the "remotely sensed" reflection point data computed from the pressure transducer array. This indicates that wave reflection is primarily from the shoreline with negligible contributions from other regions of the profile. Similar observations were made by Guza and Bowen (1976) in a laboratory examination of wave reflection on a smooth sloping beach ($\beta = 7°$). Guza and Bowen (1976) also showed that when reflection is weak

($K_r < 0.4$) the reflected waves undergo a phase shift during the process of reflection. For this reason only highly reflective wave conditions corresponding to data with peak frequencies < 0.15 Hz have been selected for analysis in Fig. 3. The observed deviation between the EDM survey and the remotely sensed data can be almost entirely attributed to irregularities in the mound and perhaps slightly subnormal angles of wave incidence.

6.2. Parameterization of wave reflection

A common approach to the parameterization of wave reflection is to relate the reflection coefficient to some form of surf similarity parameter. Common examples include; the Iribarren number (ξ), the Miche number (M), or a reciprocal form of the Iribarren number $\varepsilon = \sqrt{\pi/\xi}$ (Wright and Short, 1984). Probably the most commonly used of these parameter in the field of coastal engineering is the Iribarren number. Examples plots of K_r versus Iribarren number for the preliminary (1 : 0.82 slope, dep. 1) and final (1 : 1.55 slope, dep. 2) sloping structures are given in Fig. 4a (dep. 1) and b (dep. 2) where each data point is evaluated from one measurement record. The general

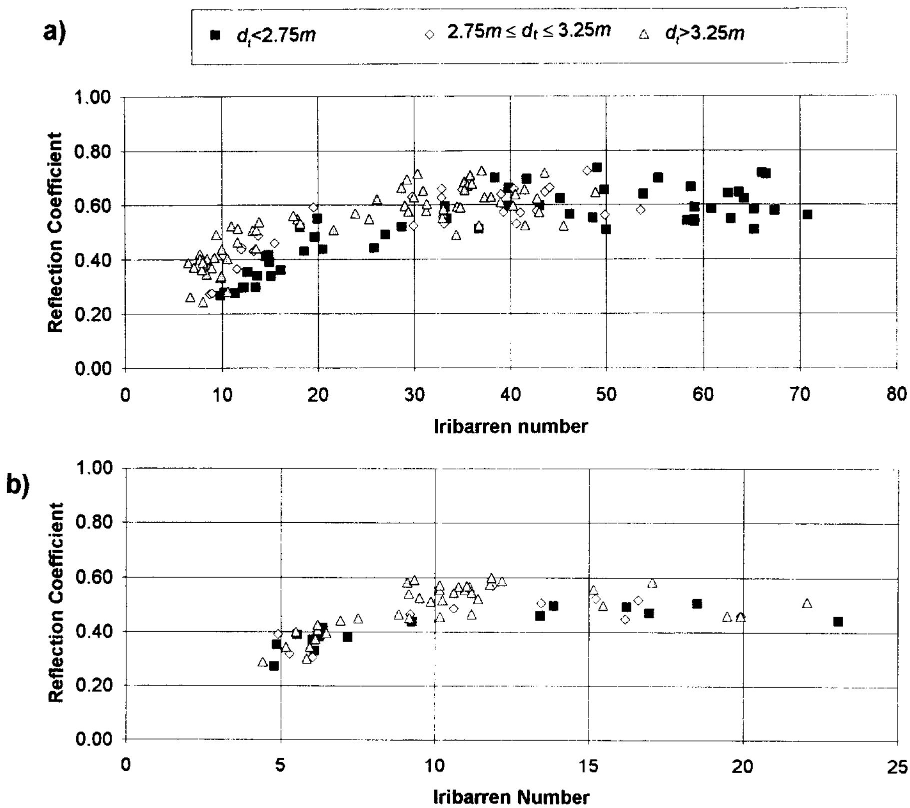

Fig. 4. Reflection coefficient as a function of Iribarren number for (a) deployment 1 ($\tan\beta = 1:0.82$) and (b) deployment 2 ($\tan\beta = 1:1.55$).

trend of the data in Fig. 4a and b shows a sharp rise in reflection at low Iribarren numbers (the breaking wave regime) until a limiting (or saturation) value of K_r is reached where further increase in ξ produces no further increase in K_r. This saturation value is related to surging wave conditions on the structure where the reduction in reflected wave energy is primarily due to factors such as wave transmission, friction and turbulence effects induced by the roughness of the structure itself rather than wave breaking. Clearly, the saturation value for K_r is lower (on average 15% less) for the modified slope (1:1.55) than the original slope (1:0.82) indicating a significant reduction in wave reflection.

Inspection of Fig. 4a and to a lesser extent Fig. 4b shows that there is a systematic increase in the reflectivity of the structure with depth (tide). This depth dependence is more evident in deployment 1 (Fig. 4a) in part due to the fact that data were collected from a broader range of water depths as a result of the transducers being mounted closer

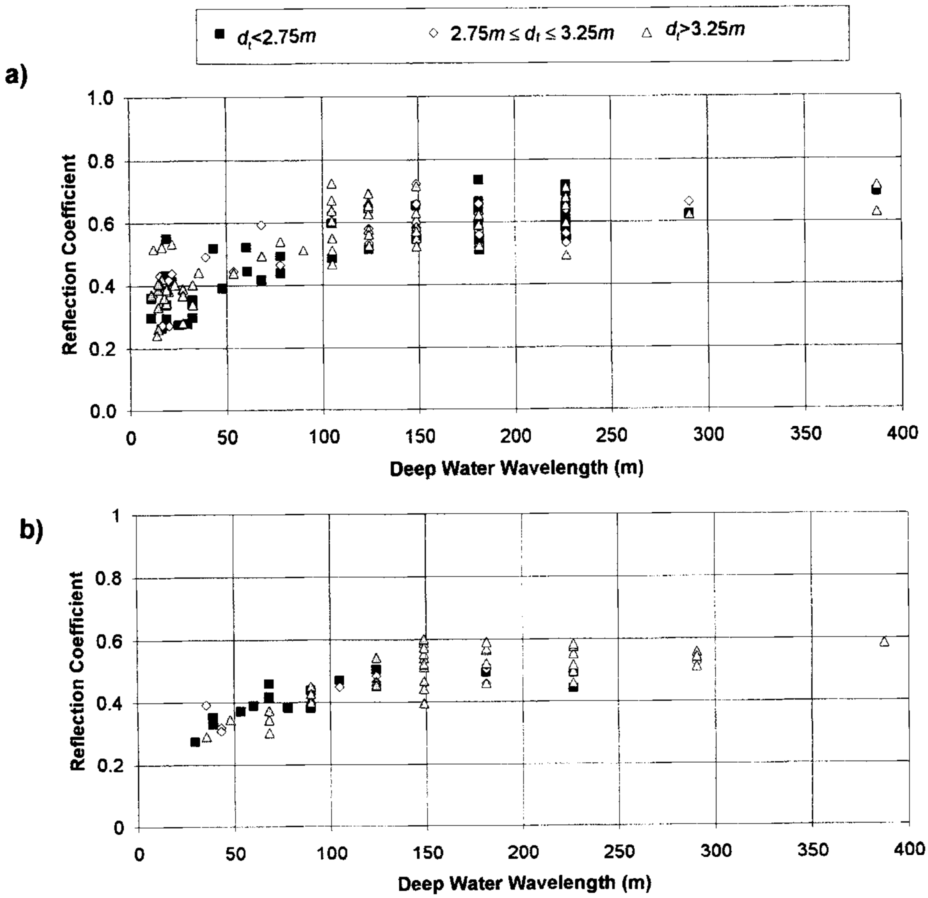

Fig. 5. Reflection coefficient as a function of deep water wavelength for (a) deployment 1 (tanβ = 1:0.82) and (b) deployment 2 (tanβ = 1:1.55).

to the sea bed. Davidson et al. (1994) postulated that the observed depth dependence was primarily due to the increasing influence of the flat beach in front of the structure which promoted wave dissipation through breaking as the water depth shallows.

Unfortunately, careful comparison of Fig. 4a with Fig. b shows that the Iribarren number fails to collapse the 2 data sets (dep. 1 and dep. 2) onto a single curve. Similar results (not shown here) were obtained when relating K_r to other non-dimensional surf-similarity parameters M and ε. The poor parameterization of wave reflection by currently available surf-similarity parameters indicates that the relative influences of L, H_i, and $\tan\beta$ are not accurately represented in these parameters, and/or that other physically significant factors have been neglected.

Due to the poor parameterization of wave reflection by the currently available surf similarity parameters it is necessary to reassess the individual effects of L, H_i, and $\tan\beta$ together with other potentially significant parameters (e.g. d_t and D).

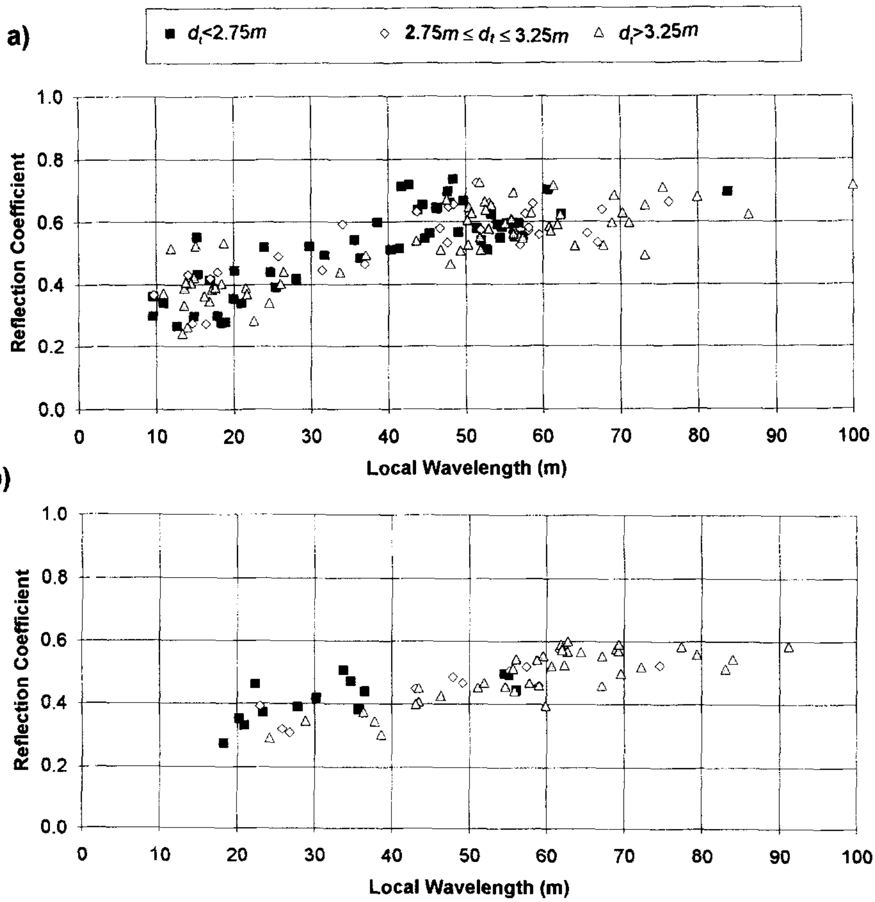

Fig. 6. Reflection coefficient as a function of local wavelength for deployment 1 ($\tan\beta = 1:0.82$) and (b) deployment 2 ($\tan\beta = 1:1.55$).

6.3. Effect of wavelength on K_r

Wavelength has a first order effect on wave reflection. The relationship between reflection coefficient and deep-water wavelength L_0 (associated with the spectral peak) is investigated in Fig. 5a (dep. 1) and b (dep. 2). The trend of the data is similar to the K_r–ξ plots discussed previously with the reflection coefficient systematically increasing in direct relation to the deep-water wavelength until a saturation level is reached. A

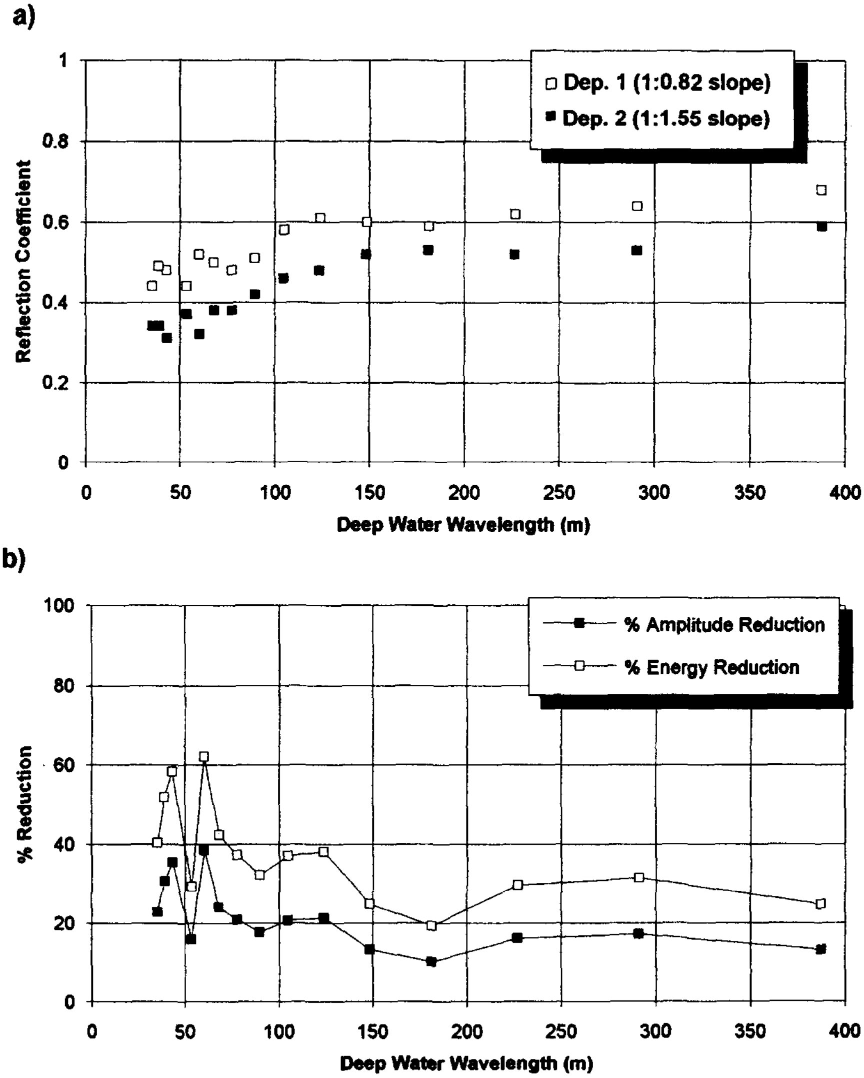

Fig. 7. (a) Average reflection coefficient for coincident deep water wavelengths, both before and after breakwater modifications. (b) Percentage reduction in reflected wave amplitude and energy versus deep water wavelength occurring as a result of the breakwater slope reduction.

similarly strong correlation of K_r with the local wavelength (L_p) evaluated at the toe of the structure is also observed, (Fig. 6a and b). The scatter seen in the data can in part be related to the variation in other physically significant variables (e.g. H_i, d_t) not considered here. Less scatter is apparent in the plots for deployment 2 (Figs. 5b and 6b) due to the narrower depth range during these measurements.

For a clearer comparison of the two deployments average values of K_r for each of the coincident L_0 values have been plotted together for both deployments (Fig. 7a). Fig. 7a clearly illustrates a significant amelioration of wave reflection due to the breakwater modification for all L_0. Another important feature illustrated by Fig. 7a is that the onset of saturation which occurs at shorter wavelengths for the steeper structure ($L_0 \approx 110$ m) than the shallower slope ($L_0 \approx 150$ m). This is as expected since one would anticipate that a wave of a given wavelength will break more readily on the shallow slope than the steep slope.

The percentage reduction in the reflection coefficient and reflected wave energy (αK_r^2) are given in Fig. 7b. Inspection of this figure shows that in the saturated region the reduction in reflected energy is of the order of 20–30%. At shorter wavelengths the percentage energy reduction is more erratic and difficult to assess due to dependencies on other parameters not accounted for here.

6.4. Multiple regression analysis

The strong dependency of K_r on L (and to some extent depth) has already been illustrated in Figs. 5 to 7. However, in order to determine more subtle relationships between K_r and other variables with weaker influences it is necessary to isolate the effect of the independent variable in question from all other variables. An effective way of achieving this is through the application of a multiple regression analysis. This technique was applied to the whole data set (including both deployments) in order to evaluate the relative importance and relationship (direct or inverse) of independent variables with the dependent variable K_r.

The review of currently available schemes for the prediction of wave reflection presented earlier indicated that the main independent variables predominantly responsible for controlling the process of wave reflection were; L, H, $\tan\beta$ and D. Data presented here has also highlighted the importance of local water depth (d).

The multiple regression analysis yields an equation relating K_r to the independent variables under consideration and the accuracy of this equation is indicated by the correlation coefficient r and the standard error σ. Regression analysis may be applied at two levels, most simply on the primary parameters (e.g. L, H, d, $\tan\beta$) or alternatively on secondary parameters (e.g. H/d, H/L, ξ) which are combinations of the primary parameters.

The procedure adopted here is to firstly carry out the regression analysis on a number of primary parameters in order to assess their relative effects on wave reflection. A number of secondary parameters are then derived on the basis of this initial analysis and the regression repeated. The use of secondary parameters fixes the relative influence of combinations of primary parameters on K_r, the success of each combination of parameters being indicated by r and σ. Although this process should not be confused with true dimensional analysis methods, the aim of this process is to combine parameters which are physically significant to the process of wave reflection, in a single non-dimensional number. If this number provides an accurate parameterization of wave reflection for both data sets (condensing all data onto a single curve) an improved predictive scheme for wave reflection will ensue. Although data were collected under widely ranging incident wave conditions the reader should note that due to the empirical nature of the approach used here and the limited range in the structural parameters (tanβ and D) such a predictive scheme will only be strictly valid for the range in conditions outlined in Table 1.

The output of the regression analysis gives K_r as follows:

$$K_r = cX_1^{p_1} X_2^{p_2} \dots X_n^{p_n} \tag{11}$$

Here X represents a primary or secondary parameter, p is a power law dependence of that parameter, c is a constant of proportionality and n the total number of parameters considered. A summary of p values for various permutations of primary and secondary parameters are shown in Table 2. The bold highlighted figures denote the focus of the analysis.

The first two rows of Table 2 deal only with the primary parameters. Row 1 gives the results of a multiple regression analysis of K_r against d_t, H_i, L_0, and cotβ. This combination of parameters indicates a highly significant correlation (at the 99% level) with a multiple regression correlation coefficient of 0.874 and a low standard error in K_r predictions of 0.054. Notice also that the regression analysis indicates that there is a direct relationship ($p > 0$, see Eq. 11) between K_r and L_0, tanβ and d_t which is consistent with results presented in Figs. 4, 5 and 7. Conversely, K_r is reduced by an increase in H_i. Although most of these relationships (except perhaps that with d_t) have been well established through laboratory tests this analysis provides valuable information as to the relative influence of these parameters. For example, since the exponent of L_0 (0.21) is approximately double the magnitude of the H_i exponent (−0.12), it would suggest a relationship of K_r with L_0^2/H_i. This is contrary to most of the currently available predictive equations which suggest a direct relationship between K_r and a reciprocal wave steepness term (L_0/H_i).

Row 1 of Table 2 yields a predictive equation for K_r of the form:

$$K_r = \frac{0.13 d_t^{0.20} L_0^{0.21}}{H_i^{0.12} \cot^{0.16}\beta} \tag{12}$$

Row 2 (Table 2) illustrates the effect of using the local wavelength L_p evaluated at the toe of the breakwater in place of L_0. Whilst the contributions of H_i and cotβ remain approximately constant the relative influence of d_t and L are adjusted quite radically. The importance of the wavelength term is increased relative to the water depth, indicating that L_p provides a more representative length scale for the incident waves in terms of wave reflection than L_o. The empirical equation resulting from row 2 of Table 2 is as follows:

$$K_r = \frac{0.10 d_t^{0.06} L_p^{0.36}}{H_i^{0.12} \cot^{0.15}\beta} \tag{13}$$

Table 2
Table of multiple regression analysis statistics. The columns of the table give different p values (see Eq. 11) for primary and secondary parameters (X). The last 3 columns represent the proportionality coefficient in Eq. 11 (c), the correlation coefficient (r) and standard error (σ) respectively. All p and c values quoted below are significant at the 95% confidence level (sample size 192 data points)

	d_t	H_i	L_0	L_p	$\cot\beta$	H_i/L_o	H_i/L_p	H_i/L_0^2	H_i/L_p^2	H_i/d_t	L_0/D	$\frac{d_t L_0^2}{H_i D^2}$	$R = \frac{d_t L_0^2}{H_i D^2 \cot\beta}$	ξ	ξ_p	ε	M	c	r	σ
1	0.197	−0.119	**0.213**		−0.155													0.131	0.874	0.054
2	0.058	−0.122		**0.362**	−0.148													0.105	0.871	0.054
3	0.261				−0.054	**0.186**												0.127	0.859	0.057
4	0.234				−0.048		**−0.238**											0.118	0.800	0.066
5	0.187				−0.171			**−0.108**										0.133	0.874	0.054
6	0.111				−0.081				**−0.167**									0.104	0.864	0.056
7	0.196	−0.119			−0.141						**0.213**							0.141	0.874	0.054
8					−0.136					**−0.124**	**0.217**							0.150	0.870	0.054
9					−0.155							**0.110**						0.152	0.870	0.054
10													**0.111**					0.151	0.868	0.055
11														**0.285**				0.219	0.738	0.074
12	0.264													**0.290**				0.160	0.796	0.067
13															**0.269**			0.254	0.610	0.087
14	0.245														**0.272**			0.191	0.670	0.082
15																**0.0004**		0.417	0.652	0.083
16	0.239															**0.0004**		0.317	0.706	0.078
17																	**−0.534**	0.857	0.735	0.075
18	0.266																**−0.534**	0.640	0.794	0.067

As one might expect since L_0 and L_p are systematically linked through the linear dispersion equation and the local water depth, correlations using Eqs. 12 and 13 are very similar ($r = 0.874$ and 0.871 respectively). This analysis indicates that if the deep water wavelength is used to characterise wave reflection, a water depth parameter should also be included in the equation.

Rows 3 to 18 in Table 2 are results of the multiple regression analysis using secondary parameters and combinations of primary and secondary parameters. Rows 3 and 4 investigate the effect of using offshore (H_i/L_0) and local (H_i/L_p) wave steepness parameters. The resulting correlation coefficient values (0.859 and 0.800) show a decrease compared to rows 1 and 2 indicating that the relative influence of H and L on wave reflection are not well described by such wave steepness terms. The lower r-value for H_i/L_p is consistent with the laboratory results by Postma (1989).

Regression of the primary parameters (rows 1 and 2) indicates that H_i and L are more appropriately combined in the form H_i/L^2. This hypothesis is explored in rows 5 and 6 of Table 2. Correlation coefficients of 0.874 (H_i/L_0^2) and 0.864 (H_i/L_p^2) indicate this hypothesis to be correct.

Numata (1976) found a strong dependence of K_r on an inverse armour diameter term in a laboratory investigation of a permeable breakwater comprised of artificial blocks (see Eq. 5). The physical significance of this term relates to; increased wave energy dissipation due to friction and turbulence (promoted by the surface roughness of the structure), and wave transmission, all of which decrease reflection and are directly related to D. Row 7 of Table 2 investigates this dependency through the introduction of a parameter relating the length scales of the waves and characteristic diameter of the mound (L_0/D). Correlation coefficients (0.874) indicate a highly significant relationship although analysis of data incorporating a much wider range of characteristic diameters is needed to confirm this result.

Row 8 combines the relative wave height term (H_i/d_t) with the relative length scale term (L_0/D) and gives a similarly high correlations ($r = 0.870$). The results of combining the relative height and length terms in a single non-dimensional number whilst maintaining the H_i/L_0^2 relation suggested by row 5 are given in row 9. Encouragingly, the correlation coefficient remains high ($r = 0.870$) and is little diminished ($r = 0.868$) through the inclusion of the structure slope term (row 10).

The analysis thus far has led to a non-dimensional number (see row 10) which for these data accurately weights the contributions of wavelength, wave height and structure slope and includes other parameters which are of importance in the process of wave reflection, namely water depth and armour diameter. Here this non-dimensional reflection parameter has been assigned the character R where:

$$R = \frac{d_t L_0^2 \tan\beta}{H_i D^2} \quad \text{Non-Dimensional Reflection Parameter} \tag{14a}$$

Comparison of this new non-dimensional reflection number with the more conventional Iribarren number yields the following relationship:

$$R = \xi\left(\frac{L_0^{1.5} d_t}{D^2\sqrt{H_i}}\right) \tag{14b}$$

Eq. 14b demonstrates the adjustment of the relative weighting of parameters in R compared to the Iribarren Number. Notice that the relative weighting of wavelength is increased, wave height is reduced and the slope remains the same. The weak dependence of reflection on wave height is supported by the laboratory observations of Postma (1989), although potentially, the influence of wave height might be increased if waves are large enough to break seawards of the structure. However, for these data wave shoaling offshore of the structure was negligible and waves broke exclusively on the structure.

The relationships between K_r and other surf-similarity parameters (ξ, ξ_p, M and ε), are investigated in rows 11 to 13. It is clear from an examination of the correlation coefficients and standard errors associated with these tests that the alternative surf similarity parameters provide a poorer representation of the process than R. This is due in all cases (rows 11 to 13) to the relative weighting given to $\tan\beta$, H and L and to the omission of the other physically significant variables d_t and D. The performance of all three alternative surf-similarity parameters are improved by the inclusion of a water depth term. Elgar et al. (1994) in their investigation of wave reflection from natural beaches found that the Miche number provided a reasonable parameterization of wave reflection. Contrary to this, data collected at Elmer indicates a poor correlation ($r =$ 0.652) of K_r with the Miche number due to an overemphasis of the effect of structure slope ($M \propto \tan^{2.5}\beta$). These correlations are not improved by isolating only the breaking wave data below saturation.

7. Discussion

7.1. Predictive schemes for wave reflection

Fig. 8 shows a comparison of K_r versus Iribarren number for both deployments (before and after the slope modification) together with some of the currently available models for the prediction of wave reflection based on laboratory tests. Since plotting K_r against Iribarren number does not effectively reduce these data to a single curve it is impossible for these models (all of which are functions of Iribarren number) to provide an accurate prediction of wave reflection for both deployments 1 and 2. Similar observations were made by Muttray et al. (1992) who comment that the large scatter in plots of K_r versus ξ for acropod and tetrapod data indicates that the Iribarren number does not represent the optimal mean for the description of the reflection process. The relative success of the various models are now examined.

The models of Seelig and Ahrens (1981), Allsop (1990) and Giménez-Curto (1979) (Eqs. 3 and 4) all predict the general trend of the data well (Fig. 8). That is to say that both data sets show a systematic increase in reflection with increase in Iribarren number until a saturation value of K_r is reached. Giménez-Curto's equation underestimates K_r for much of the data, particularly for $\xi > 20$. Conversely, Seelig and Ahrens's and Allsop's equations provide conservative estimates of K_r for $\xi < 20$ and good average saturation values for K_r for $\xi > 30$. Postma's (1989) Eq. 6 overestimates wave

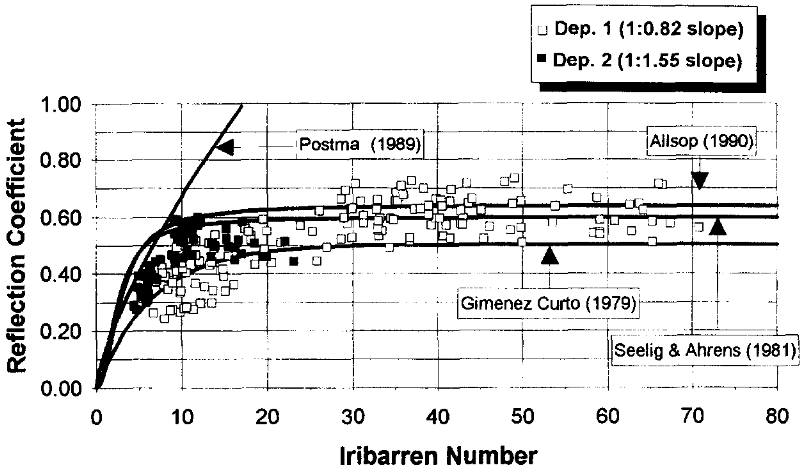

Fig. 8. Comparison of full scale field data for both deployments 1 and 2 with existing models for wave reflection.

reflection for these data over the full range of Iribarren numbers and fails to predict the limiting value for K_r at $\xi > 10$.

In the previous section multiple regression analysis was used both to develop an improved parameterization for wave reflection from two rubble mound structures in terms of the reflection parameter R (Eq. 14). From line 10 of Table 2 the resulting predictive equation is as follows:

$$K_r = 0.151 R^{0.11} \tag{15}$$

Observed and predicted reflection coefficients using Eq. 15 are shown in Fig. 9. Encouragingly, Eq. 15 seems to apply equally well to data from both deployments. However, although there is a good correlation between the observed and predicted K_r values ($r = 0.868$) with a low standard error ($\sigma = 0.055$) there seems to be a systematic "s-shaped" deviation from the straight line. Departure from the 1 : 1 line is particularly noticeable for $K_r < 0.4$. This systematic deviation between predicted and observed values largely results from the limitations inherent in an equation of the form cX^p used here.

The departure of the predicted from the observed values of K_r resulting from Eq. 15 may be reduced by incorporating the reflection parameter R in an equation which more effectively follows the trend of the data. One such equation is similar in form to that of Seelig and Ahrens (1981) (Eq. 3), where:

$$K_r = \frac{aR^{0.5}}{b + R^{0.5}} \tag{16}$$

Here a and b are empirical coefficients determined by minimising the error between observed and predicted values for K_r. Raising R to the power 0.5 in Eq. 16 leads to an

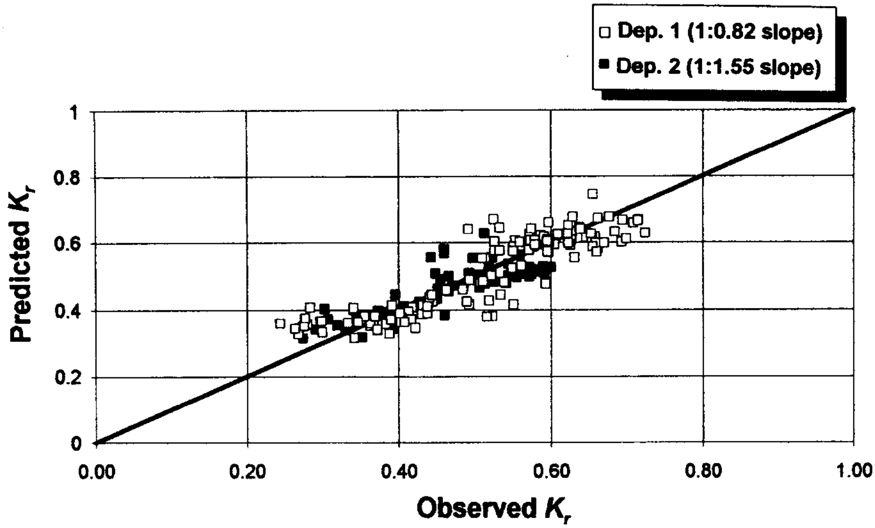

Fig. 9. Predicted (Eq. 15) versus observed reflection coefficients for deployments 1 and 2.

equivalent weighting of L_0 to that in Seelig and Ahrens' (1981) equation, but a relative reduction of the influence of H_i and $\tan\beta$, and the inclusion of depth and representative armour diameter terms. Unlike the previous plots of reflection coefficient against the Iribarren number, Fig. 10 shows that the reflection parameter R effectively converges the data onto a single curve.

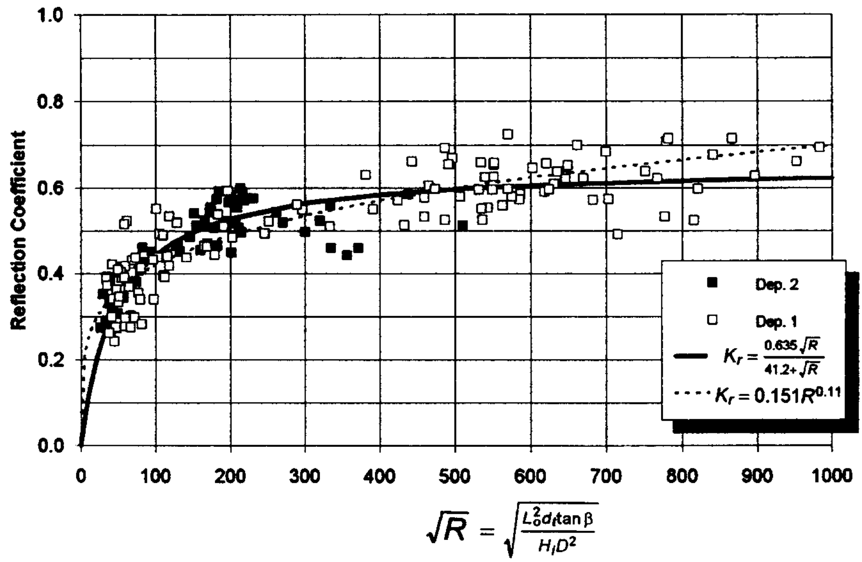

Fig. 10. Reflection coefficient versus $R^{0.5}$ for both deployments. Also shown are model predictions using Eqs. 15 and 16.

A comparison between observed reflection and estimates using Eqs. 15 (dotted line) and 16 (solid line) are also shown in Fig. 10. The scatter in the observed data about the theoretical curves is approximately consistent with the magnitude of errors in K_r of $< \pm 0.09$ due to low signal coherence between pressure sensor pairs and to oblique wave approach discussed in the data analysis section. The errors in the data over and above this value can be attributed to irregularities in the reflecting face of the structure, mild non-linearities in the data and variations in the spectral form of the incident waves.

Eq. 16 qualitatively follows the trend of the data better than Eq. 15 (Fig. 10). The relative merits of these equations for different ranges of R characterising the full range of measurements ($0 < R^{0.5} < 1000$) and a breaking wave subset ($R^{0.5} < 300$) are shown more quantitatively in Table 3. Inspection of Table 3 shows that both Eq. 15 and Eq. 16 provide accurate estimates of wave reflection over the whole range of wave conditions sampled with little difference in accuracy. There is however some suggestion that Eq. 16 provides marginally better estimates for low values of $R^{0.5}$ (< 300) which is the area of primary interest to coastal engineers, since it represents the largest, steepest waves.

The coefficient a_1 in Seelig and Ahrens's equation (Eq. 3) (and equivalently a in Eq. 16) define the upper saturation-value of the reflection coefficient. Seelig and Ahrens (1981) define a_1 as a function of wave dissipation seawards of the structure, surface roughness and multiple armour layers. Seelig and Ahrens recommend an average value of $a_1 = 0.6$ for rock or dolos structures for a conservative estimate of wave reflection. A similar analysis by Allsop (1990) gives $a_1 = 0.64$. Best fit values for a and b in Eq. 16 for these data, obtained by minimising the standard error in the predicted K_r values were 0.635 and 41.2 respectively. Thus, the saturation reflection value (a) for these data differs from Seelig and Ahrens's recommendation (a_l) by only 6%, and $< 1\%$ from Allsop's value.

Unlike, a and a_1 direct comparisons cannot be made between the coefficients b and b_1 due to the obvious differences between R and ξ. It is worthwhile mentioning however, that Seelig and Ahrens's (1981) presented evidence that b_1 increases systematically with $\cot\beta$. The regression analysis carried out here indicates that this variation in b_1 is likely to arise due to an overemphasis of the structure slope term relative to L in the Iribarren number.

Since it has been demonstrated that R provides a more accurate parameterization of K_r than previously available surf-similarity numbers, Eq. 15 or Eq. 16 will assist coastal engineers to progress towards a universal scheme for the prediction of wave reflection from porous structures. However, the input of more data from varied environments is

Table 3
Standard error (σ) and correlation coefficients (r) for reflection coefficient predictions using Eqs. 15 and 16 for different ranges of the reflection number R

Eq. No.	$R^{0.5}$-range	σ	r
16	0–1000	0.056	0.864
15	0–1000	0.055	0.868
16	0–300	0.054	0.874
15	0–300	0.056	0.864

required in order to confirm more precisely the effects of structure slope and armour diameter. Since the predictive schemes outlined in this contribution are empirical in nature they should be considered only strictly valid under the range of conditions outlined in Table 1.

7.2. *The effect of structure slope on the amelioration of wave reflection*

Of fundamental interest to the coastal engineer is the effect that the reduction of the structure's surface slope has on the amelioration of wave reflection. The economic decision to include more armour at a greater cost in order to reduce the seawards slope of the structure must be justified by the corresponding reduction in wave reflection and sediment erosion seawards of the structure.

These data have shown that the reduction of the breakwater gradient from 1 : 0.82 to 1 : 1.55 has produced a measurable and significant reduction in wave reflection. Estimates of K_r reduction computed by comparison of average saturation values obtained from the K_r vs. ξ (Fig. 4a, b) indicate a decrease of 15%. Measurements of K_r reduction vs. deep water wavelength (Fig. 7b) indicate a range in values from 10% to 20% (or 20% to 30% in energy terms) for $L_0 > 150$ m. Reduction in wave reflection below saturation is more difficult to estimate. Fig. 7b indicates that K_r is further reduced for $L_0 < 150$ m but the pattern is confused due to the complex interaction of other variables.

8. Concluding remarks

This contribution has detailed an extensive field measurement programme designed to evaluate the reflection performance of a rock island breakwater (Elmer, West Sussex, UK) both before and after modification to the seawards slope of the breakwater. The modification was designed to increase the structure stability and involved the placement of additional armour on the seawards face of the structure. This provided a unique opportunity to assess at full scale, the sensitivity of the reflection performance of the structure to variations in slope. A total of 960 data records were acquired under broadly varying incident wave conditions (Table 1), providing a data set representative of the typical wave climate at this site. The conclusions arising from this research may be summarised as follows:

(1) Under highly reflective conditions ($K_r > 0.4$) wave reflections from rubble mound breakwaters ($\tan\beta = 1:1.55$ to $1:0.82$) originated predominantly from a point close to the (time-averaged) shoreline position on the seawards face of the structure. This reflection point location moved up and down the structure profile in response to the flood and ebb of the tide. Distributed reflection from other areas of the profile was negligible.

(2) Wave reflection shows a systematic increase with Iribarren number until a saturation value of K_r is reached where further increase in ξ produces no further

increase in K_r. The slope reduction to the seawards face of the breakwater (1 : 0.82 to 1 : 1.55) results in a 15% reduction in the saturation value of K_r.

(3) Although the reflection coefficient varies systematically with the Iribarren number, plots of K_r vs. ξ fail to reduce the two data sets (before and after the slope modification) to a single curve.

(4) Multiple regression analysis of the dependent variable K_r with independent variables (L_0, H_i, d_t and $\tan\beta$) are in agreement with previous laboratory tests which suggest that K_r is directly proportional to L_0 and inversely proportional to H_i and $\tan\beta$. However, unlike previous laboratory tests this analysis has highlighted the importance of the local water depth on K_r, where reflection increases in proportion to water depth.

(5) Multiple regression analysis indicates that a wave steepness parameter (inherent in the Iribarren number) of the form H_i/L_0 or H_i/L_p unduly weights the effect of wave height over wavelength. A much stronger correlation is found between K_r and the term H_i/L_0^2.

(6) Currently available surf-similarity numbers including ξ, ε, and M fail to provide an accurate parameterization of wave reflection for these data.

(7) Multiple regression analysis of these field data suggests a more accurate parameterization of wave reflection from porous rock-armour structures is given by the non-dimensional reflection number R where;

$$R = \frac{d_t L_0^2 \tan\beta}{H_i D^2}$$

R has the advantage of more effectively weighting the relative importance of L_0, H_i and $\tan\beta$ and including other physically significant variables d_t and D. Indeed, plotting K_r vs. R (or some power of R, Fig. 10) effectively condenses the data for both structure slopes onto the same curve reinforcing this conclusion.

(8) Multiple regression analysis yields several empirical equations (see Table 2) for the prediction of wave reflection from rock island breakwaters. One of the most significant of these takes the form:

$$K_r = 0.151 R^{0.11}$$

An alternative empirical equation similar in form to Seelig and Ahrens's (1981) equation which more effectively describes the reflection process below saturation is:

$$K_r = \frac{aR^{0.5}}{b + R^{0.5}}$$

Here a and b are empirical coefficients having the values of 0.635 and 41.2 respectively. Due to the empirical nature of these equations and the limited range of structure variables (particularly D and $\tan\beta$), Eqs. 15 and 16 may only be considered strictly valid within the range of conditions during this experiment (these are summarised in Table 1). More analysis (preferably of field data to eliminate any potential scale effects) is required in order to confirm the exact influences of D and $\tan\beta$ under a broader range of these values.

Acknowledgements

The authors would like to extend their thanks to the Engineering and Physical Sciences Research Council (EPSRC, grant No. GR/H17183) for funding this research programme and to MAST (grant No. MAS2-CT92-0030) for additional funding. We would also like to acknowledge the technician support in the School of Civil and Structural Engineering (Univ. of Plymouth), and Arun District Council for their kind co-operation and support in the field.

References

Ahrens, J.P., 1980. Unpublished irregular wave reflection data. U.S. Army Corps of Engineers, Coastal Engineering Research Centre, Fort Belvoir, VA.

Ahrens, J.P. and Seelig, W.N., 1980. Wave runup on a rip-rap protected dike (unpub.). U.S. Army Corps of Engineers, Coastal Engineering Research Centre, Fort Belvoir, VA.

Allsop, N.W.H. and Channell, A.R., 1988. Wave reflections in harbours: The reflection performance of wave screens. Hydraulics Research Report OD 102.

Allsop, N.W.H. and Hettiarachchi, S.S.L., 1988. Reflections form coastal structures. In: Proc. 21st Conf. on Coastal Eng., Malaga. ASCE, New York.

Allsop, N.W.H., 1990. Reflection performance of rock armoured slopes in random waves. In: Proc. 22nd Conf. on Coastal Eng., Delft. ASCE, New York.

Battjes, J.A., 1974. A computation of set-up, longshore currents, run-up and overtopping due to wind generated waves. Ph.D. Dissertation, Delft University of Technology.

Battjes, J.A., 1975. Surf similarity. In: Proc. 14th Conf. on Coastal Eng., Copenhagen, 1974. ASCE, New York, pp. 466–480.

Bird, P.A.D. and Bullock, G.N., 1991. Field measurement of the wave climate. In: D.H. Peregrine and J.H. Loveless (Editors), Developments in Coastal Engineering. University of Bristol, pp. 13–24.

Bird, P.A.D., Davidson, M.A., Bullock, G.N. and Huntley, D.A., 1994. Wave measurement near reflective structures. In: Proc. Conf. Coastal Dynamics '94, Barcelona. ASCE, New York, pp. 701–711.

Bird, P.A.D., Davidson, M.A., Ilic, S., Bullock, G.N., Chadwich, A.J., Axe, P. and Huntley, D.A., 1995. Wave transformation and attenuation characteristics of rock island breakwaters. In: Proc Conf. Coastal Structures and Breakwaters, London.

Chesnutt, C.B., 1978. Analysis of results from 10 movable-bed experiments. Vol. VIII, MR 77-7, Laboratory effects in beach studies, U.S. Army, Corps of Eng., Coastal Eng. Res. Centre, Fort Belvoir, VA.

CIRIA/CUR, 1991. Manual on the use of rock in coastal and shoreline engineering. London, pp. 505–507.

Davidson, M.A., Bird, P.A.D., Bullock, G.N. and Huntley, D.A., 1994. Wave reflection: Field measurements, analysis and theoretical developments. In: Proc. Conf. Coastal Dynamics '94, Barcelona. ASCE, New York, pp. 642–655.

DeBok, D.E. and Sollitt, C.K., 1978. A large scale model study of placed stone breakwaters. Oregon State University, Dept. of Ocean Eng., Corvallis, OR.

Elgar, S., Herbers, T.H.C. and Guza, R.T., 1994. Reflection of ocean surface gravity waves from a natural beach. J. Phys. Oceanogr., 24: 1503–1511.

Gaillard, P., Gauthier, M. and Holly, F., 1980. Method of analysis of random wave experiments with reflecting coastal structures. In: Proc. 17th Conf. on Coastal Eng., Sydney. ASCE, New York, pp. 204–220.

Giménez-Curto, L.A., 1979. Behaviour of rubble mound breakwaters under wave action. Ph.D. Thesis, Univ. of Santander (in Spanish; see also Losada and Giménez-Curto, 1981).

Goda, Y., 1975. Irregular wave deformation in the surf zone. Coastal Eng. Jpn., 18: 13–26.

Gunbak, A.R., 1979. Rubble mound breakwater. Report No. 1, The University of Trondheim, Division of Port and Ocean Engineering, Trondheim.

Guza, R.T. and Bowen, A.J., 1976. Resonant interactions for waves breaking on a beach. In: Proc. 15th Conf. on Coastal Eng., Honolulu, HI. ASCE, New York, pp. 560–579.

Guza, R.T. and Thornton, E.B., 1980. Local and shoaled comparisons of sea surface elevations, pressures and velocities. J. Geophys. Res., 85(C3): 1524–1530.

Holland, B. and Coughlan, P., 1994. The Elmer coastal defence scheme. In: MAFF Conference for River and Coastal Engineering, Loughborough.

Kajima, R., 1969. Estimation of incident wave spectrum under the influence of reflection. Coastal Engineering in Japan, Vol. 12.

Losada, M.A. and Giménez-Curto, L.A., 1981. Flow characteristics on rough, permeable slopes under wave action. Coastal Eng., 4: 187–206.

Madsen, O.S. and White, S.M., 1976. Reflection and transmission characteristics of porous rubble-mound breakwaters. MR 76-5, U.S. Army Corps of Engineers, Coastal Engineering Research Centre, Fort Belvoir, VA.

Miche, M., 1951. Le pouvoir reflêchissant des ouvrages maritimes exposés à l'action de la houle. Ann. Ponts Chaussées, 121: 285–319.

Muttray, M., Oumeraci, H., Zimmermann, C. and Partensky, H.W., 1992. Wave energy dissipation on and in rubble mound structure. In: Proc. 23rd Conf. on Coastal Eng., Venice. ASCE, New York, pp. 1434–1447.

Numata, A., 1976. Laboratory formulation for transmission and reflection at a permeable breakwater of artificial blocks. Coastal Eng. Jpn., Vol. XIX: 47–58.

Oumeraci, H. and Partensky, H.W., 1990, Wave induced pore pressure in rubble mound breakwaters. In: Proc. 22nd Conf. on Coastal Eng., Delft. ASCE, New York.

Postma, G.M., 1989. Wave reflection from rock slopes under random wave attack. Unpublished M.Sc. Thesis, Delft Univ. of technology, 106 pp.

Seelig, W.N. and Ahrens, J.P., 1981. Estimation of wave reflection and energy dissipation coefficients for beaches, revetments and breakwaters. CERC Technical paper 81-1, Fort Belvoir, U.S. Army Engineer Waterways Coastal Experiment Station, Vicksburg, MS.

Seelig, W.N., 1980. Two-dimensional wave tests of transmission and reflection characteristics of laboratory breakwaters. TR 80-1, U.S. Army, Corps of Eng. Res. Centre, Fort Belvoir, VA.

Shimada, A., Fujimoto, T., Saito, S., Sakikiyama, T. and Hirakuchi, H., 1986. Scale effects on stability and wave reflection regarding armour units. In: Proc. 20th Coastal Eng. Conf., Taipei. ASCE, New York, Vol. 3, pp. 2238–2252.

Sollitt, C.K. and Cross, R.H., 1972. Wave transmission through permeable breakwaters. In: Proc. 13th Conf. Coastal Eng., Vancouver. ASCE, New York, pp. 1827–1846.

Sollitt, C.K. and DeBok, D.H., 1976. Large scale model tests of placed stone breakwaters. In: Proc. 15th Conf. Coastal Eng., Honolulu, HI. ASCE, New York, Vol. 3, pp. 2572–2588.

Shore Protection Manual, 1984. US Army Corps of Engineers, Waterway Experiment Station Coastal Engineering Research Centre.

Ursell, J.N., Dean, R.G. and Yu, Y.S., 1960. Forced small amplitude water waves: A comparison of theory and experiment. J. Fluid Mech., 7(1): 33–52.

Van der Meer, J.W., 1988. Rock slopes and gravel beaches under wave attack. Doctoral Thesis. Delft Univ. of Technology. Also: Delft Hydraulics Communications No. 396.

Van der Meer, J.W., 1992. Conceptual design of rubble mound breakwaters. In: Proc. of a short course on the design and reliability of coastal structures, 23rd Conf. Coastal Eng., Venice. ASCE, New York, pp. 447–510.

Wright, L.D. and Short, A.D., 1984. Morphodynamic variability of surf zones and beaches: A synthesis. Mar. Geol., 56: 93–118.